AMERICAN SOCIETY FOR MICROBIOLOGY | Journal of Bacteriology®

RESEARCH ARTICLE

Inactivation of the Pta-AckA Pathway Impairs Fitness of *Bacillus anthracis* during Overflow Metabolism

Harim I. Won,[a]* Sean M. Watson,[a]* Jong-Sam Ahn,[a] Jennifer L. Endres,[a] Kenneth W. Bayles,[a] Marat R. Sadykov[a]

[a]Department of Pathology and Microbiology, University of Nebraska Medical Center, Omaha, Nebraska, USA

Harim I. Won and Sean M. Watson contributed equally to this work. Author order was determined by drawing straws.

ABSTRACT Under conditions of glucose excess, aerobically growing bacteria predominantly direct carbon flux toward acetate fermentation, a phenomenon known as overflow metabolism or the bacterial "Crabtree effect." Numerous studies of the major acetate-generating pathway, the phosphotransacetylase (Pta)-acetate kinase (AckA) pathway, have revealed its important role in bacterial fitness through the control of central metabolism to sustain balanced growth and cellular homeostasis. In this work, we highlight the contribution of the Pta-AckA pathway to the fitness of the spore-forming bacterium *Bacillus anthracis*. We demonstrate that disruption of the Pta-AckA pathway causes drastic growth reduction in the mutants and alters the metabolic and energy status of the cells. Our results revealed that inactivation of the Pta-AckA pathway increases the glucose consumption rate, affects intracellular ATP, NAD^+, and NADH levels, and leads to a metabolic block at the pyruvate and acetyl coenzyme A (acetyl-CoA) nodes. Consequently, accumulation of intracellular acetyl-CoA and pyruvate forces bacteria to direct carbon into the tricarboxylic acid and/or glyoxylate cycles, as well as fatty acid and poly(3-hydroxybutyrate) biosynthesis pathways. Notably, the presence of phosphotransbutyrylase (Ptb) in *B. anthracis* partially compensates for the loss of Pta activity. Furthermore, overexpression of the *ptb* gene not only eliminates the negative impact of the *pta* mutation on *B. anthracis* fitness but also restores normal growth in the *pta* mutant of the non-butyrate-producing bacterium *Staphylococcus aureus*. Taken together, the results of this study demonstrate the importance of the Pta-AckA pathway for *B. anthracis* fitness by revealing its critical contribution to the maintenance of metabolic homeostasis during aerobic growth under conditions of carbon overflow.

IMPORTANCE *B. anthracis*, the etiological agent of anthrax, is a highly pathogenic, spore-forming bacterium that causes acute, life-threatening disease in both humans and livestock. A greater understanding of the metabolic determinants governing the fitness of *B. anthracis* is essential for the development of successful therapeutic and vaccination strategies aimed at lessening the potential impact of this important biodefense pathogen. This study is the first to demonstrate the vital role of the Pta-AckA pathway in preserving energy and metabolic homeostasis in *B. anthracis* under conditions of carbon overflow, thus highlighting this pathway as a potential therapeutic target for drug discovery. Overall, the results of this study provide important insights into the metabolic processes and requirements driving rapid *B. anthracis* proliferation during vegetative growth.

KEYWORDS overflow metabolism, acetate production, metabolic status, fitness, *Bacillus anthracis*

During growth on glucose and other easily metabolizable carbohydrates, various bacteria, including *Bacillus* spp., generate acetic acid as one of the most abundant

Citation Won HI, Watson SM, Ahn J-S, Endres JL, Bayles KW, Sadykov MR. 2021. Inactivation of the Pta-AckA pathway impairs fitness of *Bacillus anthracis* during overflow metabolism. J Bacteriol 203:e00660-20. https://doi.org/10.1128/JB.00660-20.

Editor Michael Y. Galperin, NCBI, NLM, National Institutes of Health

Address correspondence to Marat R. Sadykov, msadykov@unmc.edu.

* Present address: Harim I. Won, Department of Immunology and Infectious Diseases, Harvard T. H. Chan School of Public Health, Boston, Massachusetts, USA; Sean M. Watson, Department of Immunology and Infectious Diseases, Harvard T. H. Chan School of Public Health, Boston, Massachusetts, USA.

Received 30 November 2020
Accepted 4 February 2021
Accepted manuscript posted online 16 February 2021
Published 8 April 2021

by-products of carbon metabolism (1–8). The major pathway of acetate production in prokaryotes, the phosphotransacetylase (Pta)-acetate kinase (AckA) pathway, is directly linked to central metabolism and is composed of two enzymes, Pta and AckA. In *Escherichia coli* and the majority of Gram-negative bacteria, the *pta* and *ackA* genes, encoding Pta and AckA, respectively, form a single operon; in *Bacillus subtilis* and other Gram-positive bacteria, however, these genes are located at distant loci on the chromosome (2, 5, 6, 9–12). During acetate fermentation, Pta catalyzes a reaction with acetyl coenzyme A (acetyl-CoA) to generate the high-energy, acid/base-labile intermediate acetyl phosphate (AcP), which is then converted to acetate by AckA in the subsequent reaction of substrate-level phosphorylation to generate ATP (5). In anaerobically growing bacteria, the end product of glycolysis, pyruvate, undergoes mixed-acid fermentation, leading to excretion of lactate, acetate, formate, and ethanol (13–15). In the presence of oxygen, however, pyruvate is decarboxylated to acetyl-CoA by the pyruvate dehydrogenase complex (PDHC). The metabolic fate of aerobically generated acetyl-CoA depends on the growth conditions. In environments with limited glucose, acetyl-CoA is completely oxidized in the tricarboxylic acid (TCA) cycle to generate energy primarily through aerobic respiration (oxidative phosphorylation). Under conditions of glucose excess, however, the TCA cycle activity is restricted by carbon catabolite repression (16–20) and acetyl-CoA is directed into acetate fermentation, where energy is generated by the less efficient process of substrate-level phosphorylation, a phenomenon known as overflow metabolism or the bacterial "Crabtree effect" (5, 21). Overflow metabolism has been widely studied in *E. coli* and other bacteria over the decades, and numerous works have revealed the critical importance of aerobic acetate fermentation for bacterial fitness, central metabolism, cellular homeostasis, and physiology through the preservation of the intricate balance between glycolytic flux and pathways involved in energy production and biosynthesis (5, 6, 18, 22–29). To date, however, the contribution of acetate fermentation to *Bacillus anthracis* fitness and physiology during overflow metabolism is still poorly understood, and the Pta-AckA pathway in this medically important pathogen has not been characterized.

In this study, we analyzed the contribution of the Pta-AckA pathway to the fitness and physiology of *B. anthracis*. We demonstrated that disruption of either *pta* or *ackA* significantly impairs growth and affects cellular homeostasis of *B. anthracis* under conditions of carbon overflow. Our results showed that the fitness defects in the mutants were associated with a metabolic block at the pyruvate and acetyl-CoA nodes, leading to redirection of carbon away from growth into pathways that normally have only limited expression under conditions of carbon overflow.

RESULTS AND DISCUSSION

Inactivation of the Pta-AckA pathway impairs *B. anthracis* growth. During growth under conditions of glucose and oxygen excess, *Bacillus* spp. generate acetate as the major by-product of carbon overflow metabolism (1, 2, 18, 30, 31). This implies that the Pta-AckA pathway, driving carbon flux toward acetate production, can play an essential role in *B. anthracis* fitness, as has been reported for other bacteria (5–7, 10, 32–35). To determine the contribution of the Pta-AckA pathway to *B. anthracis* growth and to examine its impact on bacterial metabolic status, we inactivated the *ackA* and *pta* genes in the *B. anthracis* strain V770-NP1-R (see Materials and Methods). Disruption of the Pta-AckA pathway by inactivation of the *ackA* and *pta* genes had a negative impact on overall bacterial growth (Fig. 1A) and drastically decreased growth rates during the exponential phase in both mutants, compared to the wild-type strain (Fig. 1B). The impairment of growth was accompanied by a significant decline in the concentrations and rate of acetic acid excretion in both the *ackA* and *pta* mutants (Fig. 1C and D). Furthermore, the decreased growth rates in both mutants were reflected in the reduced temporal depletion of glucose from the culture medium (Fig. 1E) and an increase in the glucose consumption rate during the exponential growth phase (Fig. 1F). This suggests that carbon flux was directed into other metabolic pathways, similar to what has been reported for *Staphylococcus aureus* (6). Importantly, a complementation study using

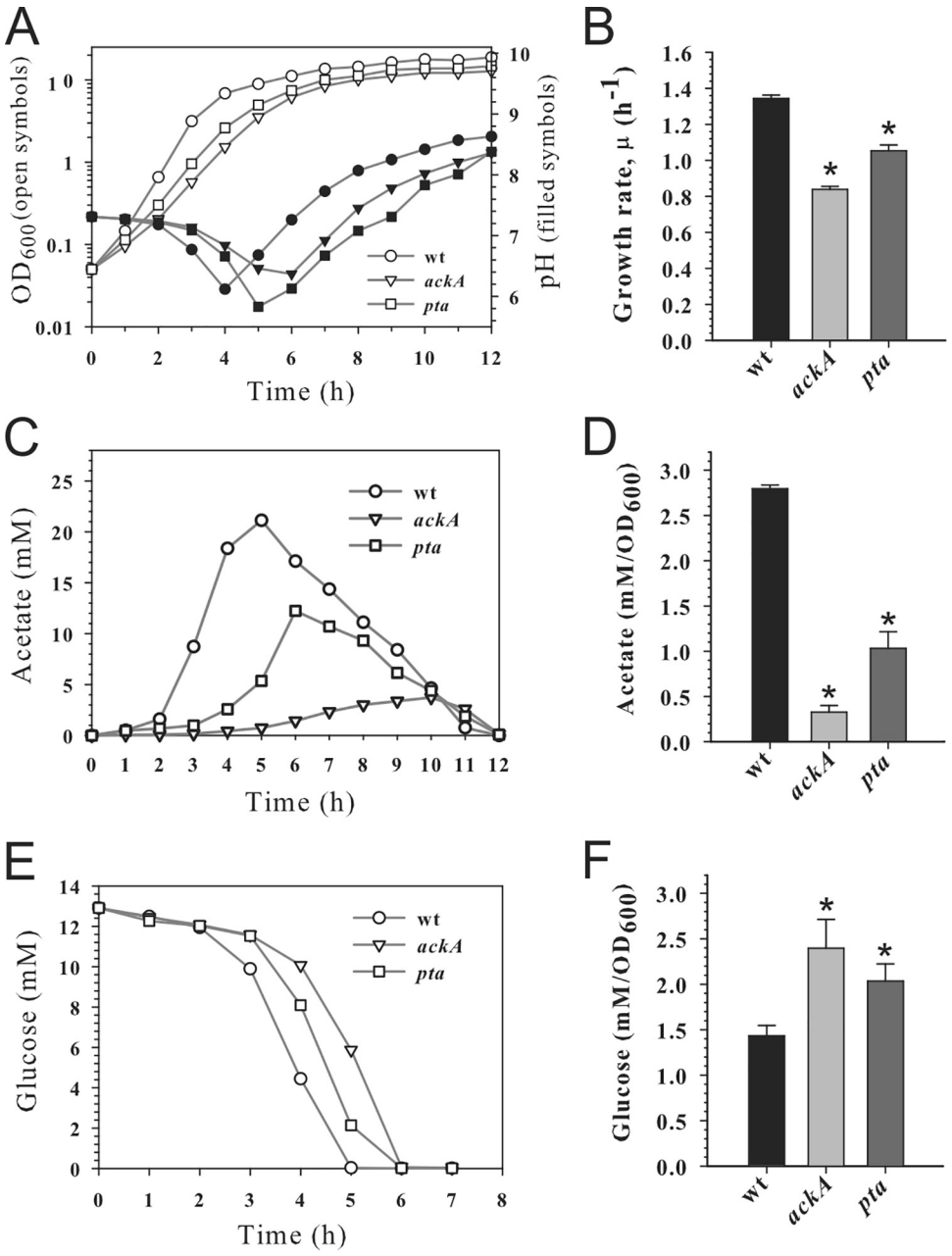

FIG 1 Inactivation of the Pta-AckA pathway affects growth characteristics of *B. anthracis*. (A) Growth curves of the wild-type (wt) strain V770-NP1-R and mutant strains V770-*ackA* and V770-*pta* grown aerobically in TSB containing 0.25% glucose. The OD_{600} and the pH of the culture medium were determined at the indicated times. (B) Growth rate of the wild-type strain V770-NP1-R and mutant strains V770-*ackA* and V770-*pta* grown aerobically in TSB containing 0.25% glucose, determined between 0 and 3 h of growth. (C) Temporal accumulation and depletion of acetic acid in the culture medium of strains V770-NP1-R, V770-*ackA*, and V770-*pta*. (D) Acetate excretion rate determined for strains V770-NP1-R, V770-*ackA*, and V770-*pta* between 0 and 3 h of growth. (E) Temporal depletion of glucose from the culture medium of strains V770-NP1-R, V770-*ackA*, and V770-*pta*. (F) Glucose consumption rate determined for strains V770-NP1-R, V770-*ackA*, and V770-*pta* between 0 and 3 h of growth. For panels A, C, and E, the results are representative of at least three independent experiments. For panels B, D, and F, the results are presented as the means plus standard errors of the means of duplicate determinations for at least three independent experiments. Statistical significance between the wild-type strain and the *pta* and *ackA* mutants was determined by using Student's *t* test. *, $P < 0.005$.

plasmids containing the wild-type alleles of the *ackA* and *pta* genes showed restoration of the growth characteristics in the mutants to the wild-type levels (see Fig. S1A and B in the supplemental material), verifying the absence of second-site mutations and confirming that the growth impairment was due to the inactivation of either *ackA* or *pta*. Taken

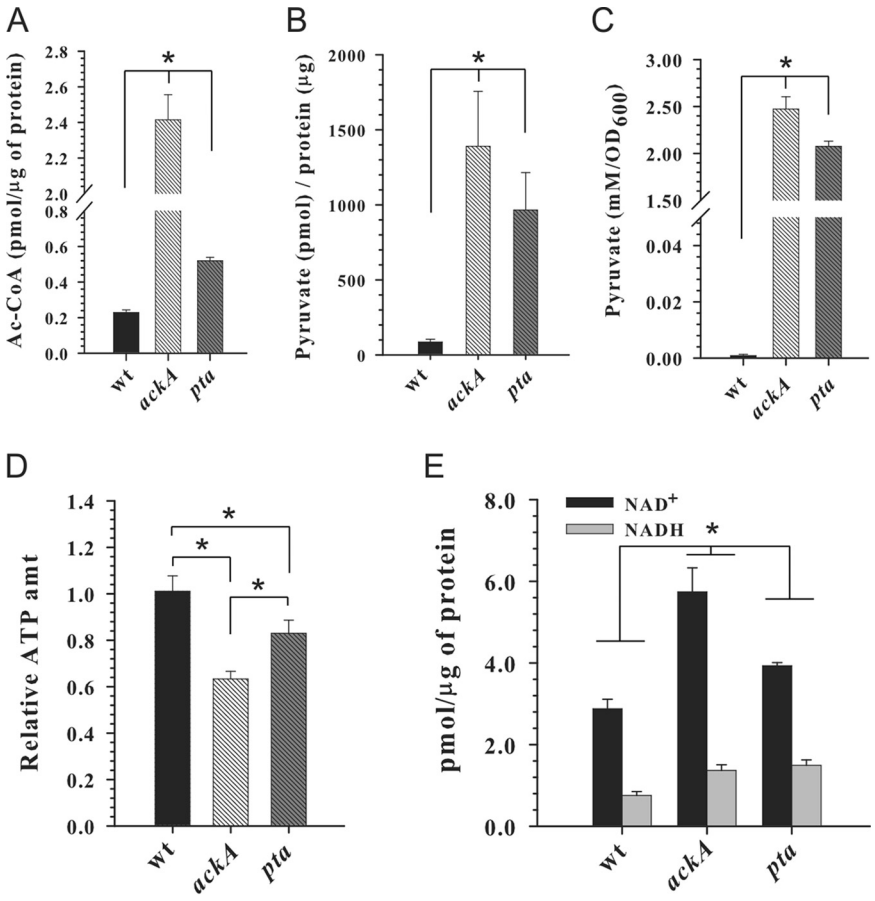

FIG 2 Inactivation of the Pta-AckA pathway alters carbon flux at the pyruvate and acetyl-CoA nodes and affects the energy status of *B. anthracis*. (A) Intracellular acetyl-CoA (Ac-CoA) concentrations determined for strains V770-NP1-R, V770-*ackA*, and V770-*pta* after 3 h of aerobic growth in TSB containing 0.25% glucose. wt, wild-type. (B) Intracellular pyruvate concentrations determined for strains V770-NP1-R, V770-*ackA*, and V770-*pta* after 3 h of aerobic growth in TSB containing 0.25% glucose. (C) Concentrations of pyruvate in the culture medium determined for strains V770-NP1-R, V770-*ackA*, and V770-*pta* after 3 h of aerobic growth in TSB containing 0.25% glucose. (D) Intracellular ATP concentrations determined for strains V770-NP1-R, V770-*ackA*, and V770-*pta* after 3 h of aerobic growth in TSB containing 0.25% glucose. (E) Intracellular NAD^+ and NADH concentrations determined for strains V770-NP1-R, V770-*ackA*, and V770-*pta* after 3 h of aerobic growth in TSB containing 0.25% glucose. The results are presented as the means plus standard errors of the means of duplicate determinations for at least three independent experiments. Statistical significance between the wild-type strain and the *pta* and *ackA* mutants was determined by using Student's *t* test. *, $P < 0.01$.

together, these results demonstrate an important contribution of the Pta-AckA pathway to *B. anthracis* fitness during overflow metabolism, as the loss of this pathway impairs bacterial proliferation and increases the glucose consumption rate, suggesting that carbon is directed away from growth into other cellular processes.

Disruption of the Pta-AckA pathway causes a metabolic block at the pyruvate and acetyl-CoA nodes and alters the cellular energy status. In previous studies, it was reported that inactivation of the Pta-AckA pathway affects the metabolic and energy status of *S. aureus* and *E. coli* by altering carbon flux through the pyruvate and acetyl-CoA nodes (6, 7, 32, 36). To determine whether inactivation of the Pta-AckA pathway in *B. anthracis* causes a similar effect on carbon flux, we measured the intracellular concentrations of acetyl-CoA and pyruvate in the wild-type and mutant strains during the exponential phase of growth. As anticipated, inactivation of the Pta-AckA pathway in *B. anthracis* during vegetative growth led to the accumulation of intracellular acetyl-CoA and pyruvate in the mutants (Fig. 2A and B). Furthermore, similar to the results reported earlier for *E. coli* and *S. aureus* (6, 10, 32, 37), measurements of the

extracellular pyruvate concentrations revealed its significant increase in the culture media for the *ackA* and *pta* mutants (Fig. 2C). Because pyruvate is an unusual by-product that is not normally excreted by the wild-type strain of *B. anthracis* under conditions of carbon overflow (Fig. 2C), its accumulation in the media might indicate leakage and/or transport of excess of pyruvate out of the cells. This suggests that the surge in the levels of intracellular pyruvate and/or acetyl-CoA caused by inactivation of the Pta-AckA pathway might have a negative impact on bacterial fitness, as was earlier proposed for *S. aureus* and *E. coli* (6, 32), thus forcing cells to excrete excess pyruvate and direct carbon into other metabolic pathways at the cost of growth.

During overflow metabolism, i.e., aerobic growth in the presence of excess glucose, the activity of the TCA cycle in bacilli is restricted by carbon catabolite repression (18, 38–40). Consequently, to support rapid cell proliferation under these conditions, a substantial part of energy in the form of ATP is generated through substrate-level phosphorylation via glycolysis and the Pta-AckA pathway (5, 41). Hence, the detrimental impact on bacterial fitness in the *pta* and *ackA* mutants could be a result of the decreased energy status of bacteria caused by the loss of the generation of two ATP molecules per glucose consumed through the Pta-AckA pathway. To determine whether disruption of the Pta-AckA pathway alters the cellular energy status, we measured the intracellular ATP, NAD^+, and NADH concentrations in the *ackA* and *pta* mutants during the exponential phase of growth. As seen in Fig. 2D, our results demonstrate that the intracellular ATP levels were indeed lower in the *pta* and *ackA* mutants, compared to the wild-type strain. In contrast, determination of the intracellular NAD^+ and NADH concentrations revealed significant increases in the pools of these metabolites (Fig. 2E), suggesting enhanced respiration in the mutants to compensate for the loss of ATP. Previously, we demonstrated that inactivation of the Pta-AckA pathway in *S. aureus* caused increases in the intracellular concentrations of ATP, NAD^+, and NADH, which resulted from redirection of carbon into the TCA cycle and enhanced oxidative phosphorylation in the mutants (6). In *B. anthracis*, however, our experiments demonstrate that disruption of the Pta-AckA pathway reduces the intracellular ATP concentrations in the mutants despite increasing the NAD^+ and NADH pools. Therefore, these results suggest that in *B. anthracis* carbon might be directed toward the less efficient energy-generating glyoxylate bypass of the TCA cycle, which is absent in *S. aureus*, and/or directed into energy-consuming cellular processes.

Inactivation of the Pta-AckA pathway directs carbon into the TCA and glyoxylate cycles, fatty acid biosynthesis, and PHB production. As mentioned above and similar to *S. aureus* (6), the loss of ATP production caused by inactivation of either *pta* or *ackA* increased the glucose consumption rate (Fig. 1F), suggesting enhanced carbon flux through the glycolytic machinery. In support of this, a quantitative real-time reverse transcriptase PCR (RT-PCR) analysis using primers specific to *pfkA*, the gene encoding the key glycolytic enzyme phosphofructokinase, showed $>$2.5-fold increases in the levels of *pfkA* mRNA transcripts in both mutants (Fig. 3A). Given that the metabolic block at the pyruvate and acetyl-CoA nodes increased the glucose consumption rate as well as intracellular NAD^+ and NADH levels in the mutants, we speculated that, similar to *S. aureus* and *E. coli* (6, 32), carbon flux in *B. anthracis* would be directed into the TCA and/or glyoxylate cycles in order to fulfill the ATP requirements through oxidative phosphorylation. To determine whether inactivation of the Pta-AckA pathway alters transcription of genes involved in the control of the TCA cycle, we performed a quantitative RT-PCR analysis using primers specific to the *citZ*, *citC*, and *sucA* genes, encoding the TCA cycle enzymes citrate synthase, isocitrate dehydrogenase, and 2-oxoglutarate dehydrogenase (E1), respectively, as well as primers specific to the *aceB* gene, encoding malate synthase of the glyoxylate bypass. Using this approach, we found that inactivation of *ackA* led to $>$2.5-fold increases in the levels of the *citZ*, *citC*, and *aceB* transcripts and $>$3.5-fold increases in the levels of the *sucA* transcripts (Fig. 3A). Although similar, a less pronounced positive impact on the accumulation of the corresponding transcript levels was observed for the *pta* mutant (Fig. 3A). To confirm that disruption of the Pta-AckA pathway directs carbon into the TCA cycle and/or the glyoxylate shunt,

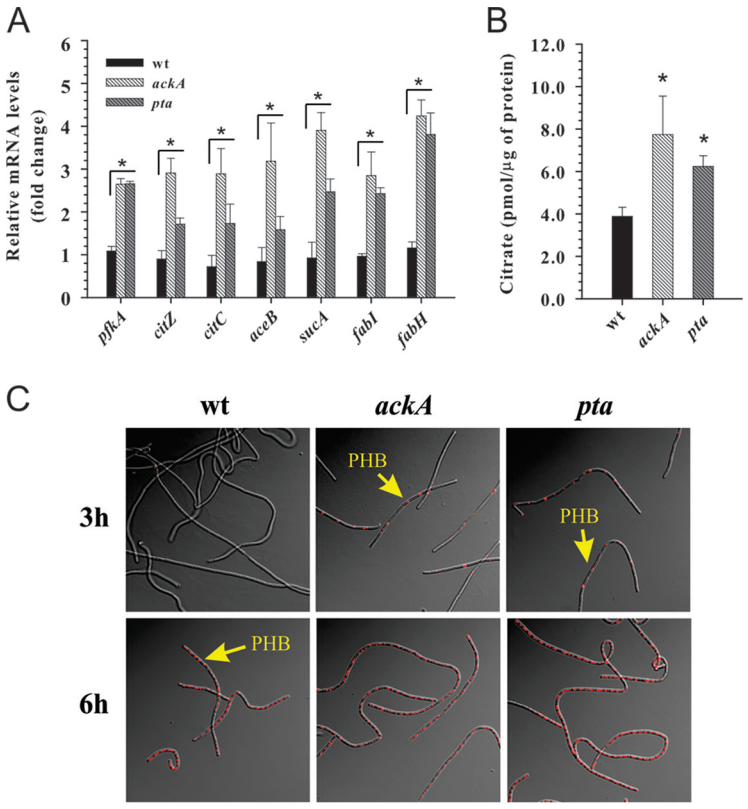

FIG 3 Inactivation of the Pta-AckA pathway in *B. anthracis* directs carbon into the TCA cycle, fatty acid biosynthesis, and PHB production. (A) Relative transcript levels of the *pfkA*, *citZ*, *citC*, *aceB*, *sucA*, *fabH*, and *fabI* genes determined by quantitative RT-PCR after 3 h of aerobic growth in TSB containing 0.25% glucose. Transcript levels in the V770-*ackA* and V770-*pta* mutants are presented as a fold difference, compared to those in the wild-type (wt) strain. (B) Intracellular citrate concentrations determined for strains V770-NP1-R, V770-*ackA*, and V770-*pta* after 3 h of aerobic growth in TSB containing 0.25% glucose. (C) Visualization of PHB granules for strains V770-NP1-R, V770-*ackA*, and V770-*pta* after 3 and 6 h of aerobic growth in TSB supplemented with 0.25% glucose by confocal laser scanning microscopy using the fluorescent dye Nile red. For panels A and B, the results are presented as the means plus standard errors of the means of duplicate determinations for at least three independent experiments. Statistical significance between the wild-type strain and the *pta* and *ackA* mutants was determined by using Student's *t* test. *, $P < 0.01$.

we measured the intracellular citrate levels in the *pta* and *ackA* mutants and the wild-type strain. In agreement with the RT-PCR data, our results showed that inactivation of the Pta-AckA pathway increased the intracellular citrate pools in both mutants, compared to the wild-type strain (Fig. 3B).

B. anthracis and other members of the *Bacillus cereus* group accumulate poly(3-hydroxybutyrate) (PHB) granules as a carbon and energy storage reservoir during growth (42). In particular, it was shown that aerobically growing *B. cereus* produced PHB through the catabolism of acetate when glucose was depleted from the medium (42, 43). In agreement with this, we previously demonstrated that in *B. anthracis* the contribution of the PHB biosynthesis pathway to carbon flux during overflow metabolism is minimal (44). Interestingly, previous studies reported that inactivation of the *pta* gene in *Ralstonia eutropha* and cyanobacteria significantly enhanced production of PHB, suggesting that the metabolic block at the acetyl-CoA node directs carbon into the PHB biosynthesis pathway (45, 46). Furthermore, overexpression of the *phbCAB* genes from *Alcaligenes eutrophus* was shown to restore the defective growth and survival of the *pta* mutant in the non-PHB-producing bacterium *E. coli* (32). Therefore, to determine whether disruption of the Pta-AckA pathway in *B. anthracis* directs carbon toward production of PHB, we visualized intracellular accumulation of PHB granules in the wild-type strain and *pta* and *ackA* mutants during the exponential (3 h) and

postexponential (6 h) phases of growth by confocal laser scanning microscopy using the fluorescent dye Nile red. In agreement with the results of previous studies (42–44), the *B. anthracis* V770-NP1-R wild-type strain produced negligible amounts of PHB during exponential growth but accumulated PHB during acetate catabolism in the postexponential phase of growth (Fig. 1C and 3C). In contrast, the *pta* and *ackA* mutants produced substantial amounts of PHB during the exponential growth phase (Fig. 3C) in the presence of glucose (Fig. 1E), suggesting that the metabolic block at the pyruvate and acetyl-CoA nodes caused by inactivation of the Pta-AckA pathway directs carbon flux toward the production of PHB, similar to findings for *R. eutropha* and cyanobacteria (45, 46).

As noted above, the intracellular ATP levels in the *pta* and *ackA* mutants were found to be lower than those in the wild-type strain under conditions of carbon overflow (Fig. 2D), suggesting that carbon is directed toward energy-consuming cellular processes. The generation of malonyl-CoA, the rate-limiting step of the *de novo* fatty acid biosynthesis catalyzed by the ATP-dependent acetyl-CoA carboxylase, represents one such energy-consuming reaction (47). To determine whether inactivation of the Pta-AckA pathway directs carbon toward lipid biosynthesis, we performed a quantitative RT-PCR analysis using primers specific to the *fabH* and *fabI* genes, which encode two key enzymes in fatty acid synthesis, i.e., β-ketoacyl-acyl carrier protein synthase III and enoyl-acyl carrier protein reductase I, respectively. Using this approach, we found that inactivation of the Pta-AckA pathway led to an $\sim$2.5-fold increase in the levels of *fabI* transcripts and a $>$3.5-fold increase in the levels of *fabH* transcripts (Fig. 3A), suggesting enhanced carbon flux toward *de novo* lipid biosynthesis in the *pta* and *ackA* mutants. It has been shown that in Gram-positive bacteria the expression of genes involved in fatty acid synthesis, including *fabH* and *fabI*, is negatively regulated by the malonyl-CoA-responsive transcriptional repressor FapR, for which malonyl-CoA serves as a concentration-dependent DNA binding inhibitor (48–50). Therefore, the observed elevated levels of the *fabH* and *fabI* mRNA transcripts not only suggest increased expression of their corresponding genes but also corroborate higher intracellular malonyl-CoA levels in the *pta* and *ackA* mutants.

Overexpression of the *ptb*-encoded Ptb restores growth of the *B. anthracis* and *S. aureus pta* mutants. Previously, it was proposed that in *B. subtilis* and *E. coli* the increase in the intracellular AcP levels might be the cause of the more severe growth inhibition seen in the *ackA* mutant, compared to the *pta* mutant (2, 35). Similarly, our current work demonstrated that inactivation of the *pta* gene in *B. anthracis* resulted in less pronounced negative impacts on bacterial growth and the metabolic status, compared to disruption of the *ackA* gene (Fig. 1, 2, and 3A and B). In contrast, our study of the Pta-AckA pathway in *S. aureus* revealed a more severe detrimental effect of the *pta* mutation on bacterial fitness, compared to inactivation of the *ackA* gene (6). Taken together, these results suggested that perturbations in the intracellular levels of AcP might not be a primary cause of the growth defect in the mutants; rather, this difference is likely based on the presence of a species-specific enzyme or pathway that compensates for the loss of the Pta function within the cells. An earlier study of Pta from *B. subtilis* showed its ability to use the short-chain fatty acid esters propionyl-CoA and butyryl-CoA (which differ from acetyl-CoA by only one and two saturated carbon atoms, respectively) as less efficient substrates for the reaction (51). More recent characterization of Pta from *Thermotoga maritima* revealed that the N-terminal amino acid sequence of the protein showed high homology to phosphotransbutyrylases (Ptbs) from *Clostridium acetobutylicum* ATCC 824 and NCIMB 8052 (52). Furthermore, Bock and colleagues (52) showed that, similar to *B. subtilis* Pta (51), the Pta from *T. maritima* not only catalyzes a reaction with acetyl-CoA but also, to a lesser extent, can use propionyl-CoA and butyryl-CoA as substrates. Similarly, Sirobhushanam and colleagues (53) recently demonstrated that the Ptb of *Listeria monocytogenes* not only catalyzes a reversible reaction with butyryl-CoA to form butyryl phosphate but also has broad substrate specificity, with different affinities for different acyl-CoA substrates. Therefore, considering the higher levels of extracellular acetate production in the *pta* mutant,

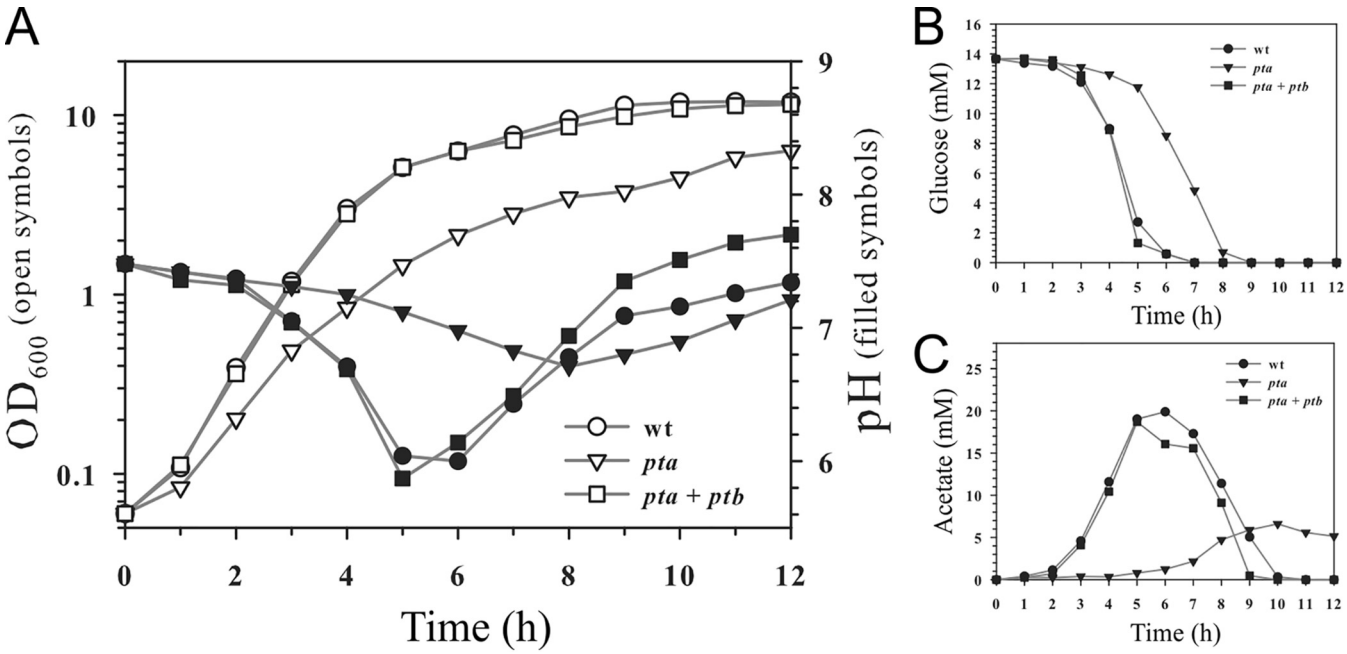

FIG 4 Overexpression of the *ptb* gene restores growth of the *pta* mutant in *S. aureus*. (A) Growth curves of the wild-type (wt) strain UAMS-1, the mutant strain UAMS-1-*pta*, and UAMS-1-*pta* with the plasmid pMRS183, containing the *ptb* gene from *B. anthracis*, grown aerobically in TSB containing 0.25% glucose. The OD_{600} and the pH of the culture medium were determined at the indicated times. (B) Temporal depletion of glucose from the culture medium of strains UAMS-1, UAMS-1-*pta*, and UAMS-1-*pta* with the plasmid pMRS183. (C) Temporal accumulation and depletion of acetic acid in the culture medium of strains UAMS-1, UAMS-1-*pta*, and UAMS-1-*pta* with the plasmid pMRS183. In the experiments, the wild-type strain and the *pta* mutant contain pCN51 (empty vector) plasmid. The results are representative of at least three independent experiments.

compared to the *ackA* mutant (Fig. 1C and D), and the ability of the Pta/Ptb family proteins to catalyze the reactions with various acyl-CoA substrates, we argued that the Ptb activity in *B. anthracis* would partially compensate for the loss of the Pta function within cells. To test this hypothesis, we constructed the plasmid pMRS183, overexpressing the Ptb of *B. anthracis* V770-NP1-R (see Materials and Methods). We then introduced this multicopy plasmid into the *pta* mutant to determine whether expression of the Ptb would complement growth. As anticipated, overexpression of Ptb restored growth of the *B. anthracis* V770-NP1-R *pta* mutant to wild-type levels (Fig. S1C). As noted earlier, a *pta* mutation in *S. aureus* caused a more severe growth defect, compared to the inactivation of *ackA* (6). Therefore, we introduced the pMRS183 plasmid into *S. aureus* strain UAMS-1, which lacks a Ptb orthologue, to determine whether expression of the *B. anthracis* Ptb would restore growth characteristics of the *pta* mutant. As shown in the Fig. 4A and B, heterologous expression of the *B. anthracis ptb* gene in *S. aureus* completely restored growth and temporal glucose consumption in the UAMS-1 *pta* mutant. Importantly, in confirmation of the ability of the *B. anthracis* Ptb to utilize acetyl-CoA as a substrate and thus to compensate for the loss of Pta function, its overexpression restored the production of acetic acid in the *pta* mutant of *S. aureus* to wild-type levels (Fig. 4C).

Concluding remarks. In this study, we demonstrated that overflow metabolism in the form of aerobic acetate excretion by *B. anthracis* represents an important physiological characteristic of this dangerous human pathogen. Our results revealed that the activity of the major acetate-generating pathway, the Pta-AckA pathway, has a direct impact on central metabolism and fitness of *B. anthracis*, as disruption of this pathway abolished rapid proliferation during exponential growth and globally altered the metabolic status of the cells. We found that the loss of ATP generation by substrate-level phosphorylation increased glucose consumption and glycolytic rates in the mutants and directed carbon into the TCA and/or glyoxylate cycles. Furthermore, our results demonstrated that inactivation of the Pta-AckA pathway resulted in a metabolic block at the pyruvate and acetyl-CoA nodes. Consequently, the surge in the intracellular

pyruvate and acetyl-CoA concentrations forced the cells to excrete pyruvate and to direct carbon away from growth toward other metabolic pathways and cellular processes that normally do not operate under these conditions. Interestingly, the fitness and metabolic differences between the *pta* and *ackA* mutants in *B. anthracis* were not associated with perturbations in the AcP pools, as suggested for other bacteria (2, 5, 35), but rather were a result of the presence of a Ptb that was able to partially compensate for the loss of Pta activity within the cells. Overall, the results of this study not only revealed the essential function of the Pta-AckA pathway in regulating cellular homeostasis by maintaining optimal carbon fluxes in central metabolism but also demonstrated the unique features of aerobic acetate production in *B. anthracis*.

MATERIALS AND METHODS

Bacterial strains, plasmids, and growth conditions. Strains and plasmids used in this study are listed in Table S1 in the supplemental material. *Escherichia coli* strains were grown in LB medium (EMD Millipore) or on LB agar. *B. anthracis strains* were grown in tryptic soy broth (TSB) (BD Biosciences) supplemented with 0.25% glucose (Sigma-Aldrich). *B. anthracis* cultures were inoculated to an optical density at 600 nm (OD_{600}) of 0.05 from overnight cultures (grown in TSB without dextrose [BD Biosciences]), incubated at 37°C, and aerated at 250 rpm with a flask/medium ratio of 10:1. Bacterial growth was assessed by measuring the OD_{600}. The OD_{600} for stationary-phase cultures was measured following dilution of cultures in TSB to remain within the linear range of a spectrophotometer. Antibiotics were purchased from Thermo Fisher Scientific and were used at the following concentrations: ampicillin, 100 μg/ml; chloramphenicol, 10 μg/ml; spectinomycin, 100 μg/ml; erythromycin, 5 μg/ml; and kanamycin, 50 μg/ml.

Construction of the *ackA* and *pta* mutants in *B. anthracis*. Primers (see Table S2 in the supplemental material) used for construction and confirmation of the *ackA* and *pta* mutations were generated based on the sequence of *B. anthracis* strain Sterne (GenBank accession number NC_005945). The *ackA* mutant was constructed by replacing a 0.6-kb internal region of the *ackA* gene with a kanamycin resistance gene (*kan*), using the gene splicing by overlap extension (SOE) technique (54). The *kan* antibiotic resistance cassette was amplified from pDG780 (55) using ackA-kan-f and ackA-kan-r primers, which contain sequences homologous to the *ackA* gene. The primers BamHI-BAS4536-f and kan-ackA-r were used for amplification of a 1.4-kb region upstream of the *ackA* gene, while a 1.2-kb region downstream of the *ackA* gene was amplified using kan-ackA-f and SalI-BAS4533-f primers. The three PCR fragments were mixed in equimolar ratio (1:1:1) and amplified using BamHI-BAS4536-f and SalI-BAS4533-f primers. The resulting 4.1-kb PCR product consisted of the 1.5-kb *kan* cassette flanked by the sequences upstream and downstream of the *ackA* gene. Following digestion with the restriction endonucleases BamHI and SalI, the 4.1-kb product was cloned into pCL52.2 (56) to generate the pMRS130 plasmid.

The *pta* mutant was constructed by replacing a 0.7-kb internal region of the *pta* gene with a spectinomycin resistance gene (*spc*), using the gene SOE technique (54). The *spc* antibiotic resistance cassette was amplified from pDG1726 (55) using pta-spc-f and pta-spc-r primers, which contain sequences homologous to the *pta* gene. The primers BamHI-BAS5239-r and spc-pta-r were used for amplification of a 1.2-kb region upstream of the *pta* gene, while a 1.1-kb region downstream of the *pta* gene was amplified using spc-pta-f and SalI-lplA-f primers. The three PCR fragments were mixed in equimolar ratio (1:1:1) and amplified using BamHI-BAS5239-r and SalI-lplA-f primers. The resulting 3.5-kb PCR product consisted of the 1.2-kb *spc* cassette flanked by the sequences upstream and downstream of the *pta* gene. Following digestion with the restriction endonucleases BamHI and SalI, the 3.5-kb product was cloned into pJA175 (44) to generate the pJM2 plasmid.

Plasmids pMRS130 and pJM2 were propagated in *E. coli* strain GM2929 (57), transformed into *B. anthracis* strain V770-NP1-R (58) by electroporation, and used to construct V770-*ackA* and V770-*pta* mutants through standard allelic exchange methodology at 37°C as described (59). The replacement of the *ackA* gene in the mutant with the *kan* cassette was confirmed by PCR using primers BAS4536-f and BAS4533-f. The replacement of the *pta* gene in the mutant with the *spc* cassette was confirmed by PCR using primers BAS5239-r and BAS5237-f.

Complementation of the *ackA* and *pta* mutations. For complementation of the *ackA* mutation, a 1.2-kb PCR product containing the wild-type *ackA* gene was amplified using primers B-SalI-ackA-f and B-SacI-ackA-r. Following digestion with the restriction endonucleases SalI and SacI, the PCR product was cloned into the plasmid pCN51 under the control of a cadmium-inducible promoter (60). The resulting recombinant plasmid was designated pMRS180. For complementation of the *pta* mutation, a 0.8-kb PCR product containing the wild-type *pta* gene was amplified using primers Ba-SalI-pta-f and B-SacI-pta-r. Following digestion with the restriction endonucleases SalI and SacI, the PCR product was cloned into the plasmid pCN51 under the control of a cadmium-inducible promoter (60). The resulting recombinant plasmid was designated pMRS200. The plasmids pMRS180 and pMRS200 were propagated in the *E. coli* strain GM2929 (57) and introduced into the V770-*ackA* and V770-*pta* mutants by electroporation correspondingly.

For heterologous complementation of the *pta* mutations in *B. anthracis* and *S. aureus* by the *B. anthracis ptb* (BAS4071) gene, a 1.0-kb PCR product containing the wild-type *ptb* gene was amplified using primers SalI-BAS4071-f and SacI-BAS4071-r. Following digestion with the restriction endonucleases SalI and SacI, the PCR product was cloned into the plasmid pCN51 under the control of a cadmium-

inducible promoter (60). The resulting recombinant plasmid was designated pMRS183. For complementation of the *pta* mutation in *B. anthracis*, the plasmid pMRS183 was propagated in *E. coli* strain GM2929 (57) and introduced into the V770-*pta* mutant by electroporation. For complementation of the *pta* mutation in *S. aureus*, the plasmid pMRS183 was transformed into strain RN4220 by electroporation and then introduced into the UAMS-1-Δ*pta* strain by phage Φ11-mediated transduction (61).

Measurement of extracellular glucose, acetic acid, and pyruvate concentrations. Aliquots of bacterial cultures (1 ml) were centrifuged at 18,407 × *g* for 3 min at 4°C. The supernatants were removed and stored at −20°C until use. Acetate and glucose concentrations were determined using kits purchased from R-Biopharm, according to the manufacturer's protocol and as described previously (6). Pyruvate concentrations were determined using the pyruvate assay kit (MBL), according to the manufacturer's protocol.

Determination of intracellular pyruvate, citrate, ATP, NAD^+, NADH, and acetyl-CoA concentrations. Intracellular pyruvate concentrations were determined using the pyruvate assay kit (MBL). Aliquots of bacterial cultures (10 ml) were harvested by centrifugation at 3,630 × *g* at 4°C for 10 min. The bacterial pellets were washed twice with 1 ml of phosphate-buffered saline (PBS) (pH 7.4), resuspended in 0.35 ml of pyruvate assay buffer, incubated for 20 min at 80°C, and lysed using Lysing Matrix B tubes (MP Biomedicals) in a FastPrep instrument (Qbiogene). The lysates were centrifuged at 18,407 × *g* at 4°C for 5 min. Pyruvate concentrations were determined according to the manufacturer's protocol and normalized to the corresponding total cellular protein concentration at the time of harvest.

Intracellular citrate concentrations were determined using the citrate colorimetric/fluorometric assay kit (BioVision). Aliquots of bacterial cultures (24 ml) were harvested by centrifugation at 3,630 × *g* at 4°C for 10 min. Bacterial pellets were washed twice with 1 ml of PBS and resuspended in 0.5 ml of PBS, followed by the addition of 0.1 ml of ice-cold 3 M perchloric acid. Cells were lysed using Lysing Matrix B tubes (MP Biomedicals) in a FastPrep instrument (Qbiogene). The lysates were then centrifuged at 18,407 × *g* for 3 min. Subsequently, 300 μl of supernatants was neutralized with 75 μl of a saturated solution of potassium bicarbonate and centrifuged at 18,407 × *g* at 4°C for 3 min. Citrate concentrations were determined according to the manufacturer's protocol and normalized to the corresponding total cellular protein concentration at the time of harvest.

Intracellular ATP concentrations were determined using the BacTiter-Glo kit (Promega) according to the manufacturer's protocol and normalized to the total cellular protein concentration at the time of harvest.

Intracellular NAD^+ and NADH concentrations were determined using the Fluoro NAD/NADH kit (Cell Technology). Aliquots of bacterial cultures (24 ml) were harvested by centrifugation at 3,630 × *g* at 4°C for 10 min. The bacterial pellets were washed twice with 1 ml of PBS and then resuspended in 0.2 ml of the NAD/NADH extraction buffer and 0.2 ml of the lysis buffer. Cells were lysed using Lysing Matrix B tubes (MP Biomedicals) in a FastPrep instrument (Qbiogene). The lysates were then incubated at 60°C for 15 min and centrifuged at 18,407 × *g* at 4°C for 3 min. NAD^+ and NADH concentrations in the lysates were determined according to the manufacturer's protocol and normalized to the total cellular protein concentration at the time of harvest.

Intracellular acetyl-CoA concentrations were determined using the PicoProbe acetyl-CoA assay kit (BioVision). Aliquots of bacterial cultures (24 ml) were harvested by centrifugation at 3,630 × *g* at 4°C for 10 min. The bacterial pellets were washed twice with 1 ml of PBS and resuspended in 0.5 ml of PBS, followed by the addition of 0.1 ml of ice-cold 3 M perchloric acid. The cells were lysed using Lysing Matrix B tubes (MP Biomedicals) in a FastPrep instrument (Qbiogene). The lysates were centrifuged at 18,407 × *g* at 4°C for 3 min. Subsequently, 300 μl of supernatants was neutralized with 75 μl of a saturated solution of potassium bicarbonate and centrifuged at 18,407 × *g* at 4°C for 3 min. Acetyl-CoA concentrations were determined according to the manufacturer's protocol and normalized to the total cellular protein concentration at the time of harvest.

All assays were performed in duplicate for at least three independent experiments. Protein concentrations for all assays were determined by the Lowry method (62).

Confocal microscopy. PHB granules in *B. anthracis* were visualized with the fluorescent dye Nile red (Sigma-Aldrich) as described (63). Bacterial samples collected after 3 and 6 h of growth in TSB supplemented with 0.25% glucose were stained with Nile red by addition of 0.5 volumes of Nile red solution (1 μg/ml in ethanol). Bacteria were immobilized by addition of 1 volume of 1% agarose (55°C), and then 15 μl of the cell suspension was placed on a microscope slide and covered with a coverslip. Bacteria were imaged with an inverted Zeiss 510 Meta confocal laser scanning microscope fitted with a Plan-Apochromat 63×/1.40 numerical aperture oil differential interference contrast (DIC) M27 objective set to a 1.7 digital zoom. In addition to the acquisition of DIC images, a 561-nm diode-pumped solid-state (DPSS) laser was used to excite Nile red and the emissions were collected with a 575- to 615-nm bandpass filter.

mRNA quantification. RNA isolation from *B. anthracis* cultures after 3 h of growth in TSB supplemented with 0.25% glucose was carried out as described previously (64). Quantitative real-time PCR was performed using *rpoD*-, *citZ*-, *citC*-, *sucA*-, *aceB*-, *fabI*-, *fabH*-, and *pfkA*-specific primers, as listed in Table S2. Briefly, cDNA was synthesized from 500 ng of total RNA using the QuantiTect reverse transcription kit (Qiagen). The samples were then diluted 1:50, and the cDNA products were amplified using the LightCycler FastStart DNA Master SYBR green I kit (Roche Applied Science) following the manufacturer's protocol. The relative transcript levels were calculated using the comparative threshold cycle (C_T) method (65) with normalization to the amount of *rpoD* transcripts. The results were recorded in duplicate and are representative of three independent experiments.

SUPPLEMENTAL MATERIAL

Supplemental material is available online only.

SUPPLEMENTAL FILE 1, PDF file, 0.7 MB.

ACKNOWLEDGMENTS

H.I.W. and S.M.W. were supported by National Institute for General Medical Science INBRE grant P20GM103427.

We declare no conflicts of interest.

REFERENCES

1. Speck EL, Freese E. 1973. Control of metabolite secretion in *Bacillus subtilis*. J Gen Microbiol 78:261–275. https://doi.org/10.1099/00221287-78-2-261.
2. Presecan-Siedel E, Galinier A, Longin R, Deutscher J, Danchin A, Glaser P, Martin-Verstraete I. 1999. Catabolite regulation of the *pta* gene as part of carbon flow pathways in *Bacillus subtilis*. J Bacteriol 181:6889–6897. https://doi.org/10.1128/JB.181.22.6889-6897.1999.
3. Kim JN, Ahn SJ, Burne RA. 2015. Genetics and physiology of acetate metabolism by the Pta-Ack pathway of *Streptococcus mutans*. Appl Environ Microbiol 81:5015–5025. https://doi.org/10.1128/AEM.01160-15.
4. Bernal V, Castano-Cerezo S, Canovas M. 2016. Acetate metabolism regulation in *Escherichia coli*: carbon overflow, pathogenicity, and beyond. Appl Microbiol Biotechnol 100:8985–9001. https://doi.org/10.1007/s00253-016-7832-x.
5. Wolfe AJ. 2005. The acetate switch. Microbiol Mol Biol Rev 69:12–50. https://doi.org/10.1128/MMBR.69.1.12-50.2005.
6. Sadykov MR, Thomas VC, Marshall DD, Wenstrom CJ, Moormeier DE, Widhelm TJ, Nuxoll AS, Powers R, Bayles KW. 2013. Inactivation of the Pta-AckA pathway causes cell death in *Staphylococcus aureus*. J Bacteriol 195:3035–3044. https://doi.org/10.1128/JB.00042-13.
7. Marshall DD, Sadykov MR, Thomas VC, Bayles KW, Powers R. 2016. Redox imbalance underlies the fitness defect associated with inactivation of the Pta-AckA pathway in *Staphylococcus aureus*. J Proteome Res 15:1205–1212. https://doi.org/10.1021/acs.jproteome.5b01089.
8. Hunt KA, Flynn JM, Naranjo B, Shikhare ID, Gralnick JA. 2010. Substrate-level phosphorylation is the primary source of energy conservation during anaerobic respiration of *Shewanella oneidensis* strain MR-1. J Bacteriol 192:3345–3351. https://doi.org/10.1128/JB.00090-10.
9. Latimer MT, Ferry JG. 1993. Cloning, sequence analysis, and hyperexpression of the genes encoding phosphotransacetylase and acetate kinase from *Methanosarcina thermophila*. J Bacteriol 175:6822–6829. https://doi.org/10.1128/jb.175.21.6822-6829.1993.
10. Kakuda H, Shiroishi K, Hosono K, Ichihara S. 1994. Construction of Pta-Ack pathway deletion mutants of *Escherichia coli* and characteristic growth profiles of the mutants in a rich medium. Biosci Biotechnol Biochem 58:2232–2235. https://doi.org/10.1271/bbb.58.2232.
11. Singh-Wissmann K, Ferry JG. 1995. Transcriptional regulation of the phosphotransacetylase-encoding and acetate kinase-encoding genes (*pta* and *ack*) from *Methanosarcina thermophila*. J Bacteriol 177:1699–1702. https://doi.org/10.1128/jb.177.7.1699-1702.1995.
12. Fraser CM, Gocayne JD, White O, Adams MD, Clayton RA, Fleischmann RD, Bult CJ, Kerlavage AR, Sutton G, Kelley JM, Fritchman RD, Weidman JF, Small KV, Sandusky M, Fuhrmann J, Nguyen D, Utterback TR, Saudek DM, Phillips CA, Merrick JM, Tomb JF, Dougherty BA, Bott KF, Hu PC, Lucier TS, Peterson SN, Smith HO, Hutchison CA, III, Venter JC. 1995. The minimal gene complement of *Mycoplasma genitalium*. Science 270:397–403. https://doi.org/10.1126/science.270.5235.397.
13. Sawers RG, Blokesch M, Bock A. 2004. Anaerobic formate and hydrogen metabolism. EcoSal Plus https://doi.org/10.1128/ecosalplus.3.5.4.
14. Nakano MM, Dailly YP, Zuber P, Clark DP. 1997. Characterization of anaerobic fermentative growth of *Bacillus subtilis*: identification of fermentation end products and genes required for growth. J Bacteriol 179:6749–6755. https://doi.org/10.1128/jb.179.21.6749-6755.1997.
15. Strasters KC, Winkler KC. 1963. Carbohydrate metabolism of *Staphylococcus aureus*. J Gen Microbiol 33:213–229. https://doi.org/10.1099/00221287-33-2-213.
16. Warner JB, Lolkema JS. 2003. CcpA-dependent carbon catabolite repression in bacteria. Microbiol Mol Biol Rev 67:475–490. https://doi.org/10.1128/mmbr.67.4.475-490.2003.
17. Gorke B, Stulke J. 2008. Carbon catabolite repression in bacteria: many ways to make the most out of nutrients. Nat Rev Microbiol 6:613–624. https://doi.org/10.1038/nrmicro1932.
18. Sonenshein AL. 2007. Control of key metabolic intersections in *Bacillus subtilis*. Nat Rev Microbiol 5:917–927. https://doi.org/10.1038/nrmicro1772.
19. Seidl K, Muller S, Francois P, Kriebitzsch C, Schrenzel J, Engelmann S, Bischoff M, Berger-Bachi B. 2009. Effect of a glucose impulse on the CcpA regulon in *Staphylococcus aureus*. BMC Microbiol 9:95. https://doi.org/10.1186/1471-2180-9-95.
20. Sadykov MR, Hartmann T, Mattes TA, Hiatt M, Jann NJ, Zhu Y, Ledala N, Landmann R, Herrmann M, Rohde H, Bischoff M, Somerville GA. 2011. CcpA coordinates central metabolism and biofilm formation in *Staphylococcus epidermidis*. Microbiology (Reading) 157:3458–3468. https://doi.org/10.1099/mic.0.051243-0.
21. Crabtree HG. 1929. Observations on the carbohydrate metabolism of tumours. Biochem J 23:536–545. https://doi.org/10.1042/bj0230536.
22. Han K, Lim HC, Hong J. 1992. Acetic acid formation in *Escherichia coli* fermentation. Biotechnol Bioeng 39:663–671. https://doi.org/10.1002/bit.260390611.
23. Farmer WR, Liao JC. 1997. Reduction of aerobic acetate production by *Escherichia coli*. Appl Environ Microbiol 63:3205–3210. https://doi.org/10.1128/AEM.63.8.3205-3210.1997.
24. Majewski RA, Domach MM. 1990. Simple constrained-optimization view of acetate overflow in *E. coli*. Biotechnol Bioeng 35:732–738. https://doi.org/10.1002/bit.260350711.
25. Varma A, Palsson BO. 1994. Stoichiometric flux balance models quantitatively predict growth and metabolic by-product secretion in wild-type *Escherichia coli* W3110. Appl Environ Microbiol 60:3724–3731. https://doi.org/10.1128/AEM.60.10.3724-3731.1994.
26. Vemuri GN, Altman E, Sangurdekar DP, Khodursky AB, Eiteman MA. 2006. Overflow metabolism in *Escherichia coli* during steady-state growth: transcriptional regulation and effect of the redox ratio. Appl Environ Microbiol 72:3653–3661. https://doi.org/10.1128/AEM.72.5.3653-3661.2006.
27. Nahku R, Valgepea K, Lahtvee PJ, Erm S, Abner K, Adamberg K, Vilu R. 2010. Specific growth rate dependent transcriptome profiling of *Escherichia coli* K12 MG1655 in accelerostat cultures. J Biotechnol 145:60–65. https://doi.org/10.1016/j.jbiotec.2009.10.007.
28. Basan M, Hui S, Okano H, Zhang Z, Shen Y, Williamson JR, Hwa T. 2015. Overflow metabolism in *Escherichia coli* results from efficient proteome allocation. Nature 528:99–104. https://doi.org/10.1038/nature15765.
29. Szenk M, Dill KA, de Graff AMR. 2017. Why do fast-growing bacteria enter overflow metabolism? Testing the membrane real estate hypothesis. Cell Syst 5:95–104. https://doi.org/10.1016/j.cels.2017.06.005.
30. Hanson RS, Srinivasan VR, Halvorson HO. 1963. Biochemistry of sporulation. I. Metabolism of acetate by vegetative and sporulating cells. J Bacteriol 85:451–460. https://doi.org/10.1128/JB.85.2.451-460.1963.
31. Nakata HM, Halvorson HO. 1960. Biochemical changes occurring during growth and sporulation of *Bacillus cereus*. J Bacteriol 80:801–810. https://doi.org/10.1128/JB.80.6.801-810.1960.
32. Chang DE, Shin S, Rhee JS, Pan JG. 1999. Acetate metabolism in a *pta* mutant of *Escherichia coli* W3110: importance of maintaining acetyl coenzyme A flux for growth and survival. J Bacteriol 181:6656–6663. https://doi.org/10.1128/JB.181.21.6656-6663.1999.
33. Rucker N, Billig S, Bucker R, Jahn D, Wittmann C, Bange FC. 2015. Acetate dissimilation and assimilation in *Mycobacterium tuberculosis* depend on carbon availability. J Bacteriol 197:3182–3190. https://doi.org/10.1128/JB.00259-15.
34. Grundy FJ, Waters DA, Allen SH, Henkin TM. 1993. Regulation of the *Bacillus subtilis* acetate kinase gene by CcpA. J Bacteriol 175:7348–7355. https://doi.org/10.1128/jb.175.22.7348-7355.1993.

35. Schutze A, Benndorf D, Puttker S, Kohrs F, Bettenbrock K. 2020. The impact of *ackA*, *pta*, and *ackA-pta* mutations on growth, gene expression and protein acetylation in *Escherichia coli* K-12. Front Microbiol 11:233. https://doi.org/10.3389/fmicb.2020.00233.
36. Yang YT, Bennett GN, San KY. 1999. Effect of inactivation of *nuo* and *ackA-pta* on redistribution of metabolic fluxes in *Escherichia coli*. Biotechnol Bioeng 65:291–297. https://doi.org/10.1002/(SICI)1097-0290(19991105)65:3<291::AID-BIT6>3.0.CO;2-F.
37. Dittrich CR, Vadali RV, Bennett GN, San KY. 2005. Redistribution of metabolic fluxes in the central aerobic metabolic pathway of *E. coli* mutant strains with deletion of the *ackA-pta* and *poxB* pathways for the synthesis of isoamyl acetate. Biotechnol Prog 21:627–631. https://doi.org/10.1021/bp049730r.
38. Tobisch S, Zuhlke D, Bernhardt J, Stulke J, Hecker M. 1999. Role of CcpA in regulation of the central pathways of carbon catabolism in *Bacillus subtilis*. J Bacteriol 181:6996–7004. https://doi.org/10.1128/JB.181.22.6996-7004.1999.
39. Kim HJ, Roux A, Sonenshein AL. 2002. Direct and indirect roles of CcpA in regulation of *Bacillus subtilis* Krebs cycle genes. Mol Microbiol 45:179–190. https://doi.org/10.1046/j.1365-2958.2002.03003.x.
40. van der Voort M, Kuipers OP, Buist G, de Vos WM, Abee T. 2008. Assessment of CcpA-mediated catabolite control of gene expression in *Bacillus cereus* ATCC 14579. BMC Microbiol 8:62. https://doi.org/10.1186/1471-2180-8-62.
41. Amarasingham CR, Davis BD. 1965. Regulation of α-ketoglutarate dehydrogenase formation in *Escherichia coli*. J Biol Chem 240:3664–3668. https://doi.org/10.1016/S0021-9258(18)97196-6.
42. Kominek LA, Halvorson HO. 1965. Metabolism of poly-β-hydroxybutyrate and acetoin in *Bacillus cereus*. J Bacteriol 90:1251–1259. https://doi.org/10.1128/JB.90.5.1251-1259.1965.
43. Nakata HM. 1966. Role of acetate in sporogenesis of *Bacillus cereus*. J Bacteriol 91:784–788. https://doi.org/10.1128/JB.91.2.784-788.1966.
44. Sadykov MR, Ahn JS, Widhelm TJ, Eckrich VM, Endres JL, Driks A, Rutkowski GE, Wingerd KL, Bayles KW. 2017. Poly(3-hydroxybutyrate) fuels the tricarboxylic acid cycle and de novo lipid biosynthesis during *Bacillus anthracis* sporulation. Mol Microbiol 104:793–803. https://doi.org/10.1111/mmi.13665.
45. Miyake M, Miyamoto C, Schnackenberg J, Kurane R, Asada Y. 2000. Phosphotransacetylase as a key factor in biological production of polyhydroxybutyrate. Appl Biochem Biotechnol 84-86:1039–1044. https://doi.org/10.1385/ABAB:84-86:1-9:1039.
46. Miyake M, Takase K, Narato M, Khatipov E, Schnackenberg J, Shirai M, Kurane R, Asada Y. 2000. Polyhydroxybutyrate production from carbon dioxide by cyanobacteria. Appl Biochem Biotechnol 84-86:991–1002. https://doi.org/10.1385/ABAB:84-86:1-9:991.
47. Tong L. 2005. Acetyl-coenzyme A carboxylase: crucial metabolic enzyme and attractive target for drug discovery. Cell Mol Life Sci 62:1784–1803. https://doi.org/10.1007/s00018-005-5121-4.
48. Schujman GE, Guerin M, Buschiazzo A, Schaeffer F, Llarrull LI, Reh G, Vila AJ, Alzari PM, de Mendoza D. 2006. Structural basis of lipid biosynthesis regulation in Gram-positive bacteria. EMBO J 25:4074–4083. https://doi.org/10.1038/sj.emboj.7601284.
49. Fujita Y, Matsuoka H, Hirooka K. 2007. Regulation of fatty acid metabolism in bacteria. Mol Microbiol 66:829–839. https://doi.org/10.1111/j.1365-2958.2007.05947.x.
50. Ellis JM, Wolfgang MJ. 2012. A genetically encoded metabolite sensor for malonyl-CoA. Chem Biol 19:1333–1339. https://doi.org/10.1016/j.chembiol.2012.08.018.
51. Rado TA, Hoch JA. 1973. Phosphotransacetylase from *Bacillus subtilis*: purification and physiological studies. Biochim Biophys Acta 321:114–125. https://doi.org/10.1016/0005-2744(73)90065-X.
52. Bock A-K, Glasemacher J, Schmidt R, Schönheit P. 1999. Purification and characterization of two extremely thermostable enzymes, phosphate acetyltransferase and acetate kinase, from the hyperthermophilic eubacterium *Thermotoga maritima*. J Bacteriol 181:1861–1867. https://doi.org/10.1128/JB.181.6.1861-1867.1999.
53. Sirobhushanam S, Galva C, Sen S, Wilkinson BJ, Gatto C. 2016. Broad substrate specificity of phosphotransbutyrylase from *Listeria monocytogenes*: a potential participant in an alternative pathway for provision of acyl CoA precursors for fatty acid biosynthesis. Biochim Biophys Acta 1861:1102–1110. https://doi.org/10.1016/j.bbalip.2016.06.003.
54. Horton RM, Cai ZL, Ho SN, Pease LR. 1990. Gene splicing by overlap extension: tailor-made genes using the polymerase chain reaction. Biotechniques 8:528–535.
55. Guerout-Fleury AM, Shazand K, Frandsen N, Stragier P. 1995. Antibiotic-resistance cassettes for *Bacillus subtilis*. Gene 167:335–336. https://doi.org/10.1016/0378-1119(95)00652-4.
56. Sau S, Sun J, Lee CY. 1997. Molecular characterization and transcriptional analysis of type 8 capsule genes in *Staphylococcus aureus*. J Bacteriol 179:1614–1621. https://doi.org/10.1128/jb.179.5.1614-1621.1997.
57. Palmer BR, Marinus MG. 1994. The *dam* and *dcm* strains of *Escherichia coli*: a review. Gene 143:1–12. https://doi.org/10.1016/0378-1119(94)90597-5.
58. Wright GG, Puziss M, Neely WB. 1962. Studies on immunity in anthrax. IX. Effect of variations in cultural conditions on elaboration of protective antigen by strains of *Bacillus anthracis*. J Bacteriol 83:515–522. https://doi.org/10.1128/JB.83.3.515-522.1962.
59. Ahn JS, Chandramohan L, Liou LE, Bayles KW. 2006. Characterization of CidR-mediated regulation in *Bacillus anthracis* reveals a previously undetected role of S-layer proteins as murein hydrolases. Mol Microbiol 62:1158–1169. https://doi.org/10.1111/j.1365-2958.2006.05433.x.
60. Charpentier E, Anton AI, Barry P, Alfonso B, Fang Y, Novick RP. 2004. Novel cassette-based shuttle vector system for Gram-positive bacteria. Appl Environ Microbiol 70:6076–6085. https://doi.org/10.1128/AEM.70.10.6076-6085.2004.
61. Novick RP. 1991. Genetic systems in staphylococci. Methods Enzymol 204:587–636. https://doi.org/10.1016/0076-6879(91)04029-n.
62. Lowry OH, Rosebrough NJ, Farr AL, Randall RJ. 1951. Protein measurement with the Folin phenol reagent. J Biol Chem 193:265–275. https://doi.org/10.1016/S0021-9258(19)52451-6.
63. Jendrossek D, Selchow O, Hoppert M. 2007. Poly(3-hydroxybutyrate) granules at the early stages of formation are localized close to the cytoplasmic membrane in *Caryophanon latum*. Appl Environ Microbiol 73:586–593. https://doi.org/10.1128/AEM.01839-06.
64. Sadykov MR, Olson ME, Halouska S, Zhu Y, Fey PD, Powers R, Somerville GA. 2008. Tricarboxylic acid cycle-dependent regulation of *Staphylococcus epidermidis* polysaccharide intercellular adhesin synthesis. J Bacteriol 190:7621–7632. https://doi.org/10.1128/JB.00806-08.
65. Schmittgen TD, Livak KJ. 2008. Analyzing real-time PCR data by the comparative *CT* method. Nat Protoc 3:1101–1108. https://doi.org/10.1038/nprot.2008.73.